SENSITIVE LASER INTERFEROMETER FOR ACOUSTIC EMISSION AND ULTRASONIC NDE

C. Harvey Palmer

Dept. of Electrical Engineering and Computer Science
and Center for Nondestructive Evaluation
The Johns Hopkins University, Baltimore, MD 21218

INTRODUCTION

Laser interferometry has important advantages for studies of acoustic emission and for ultrasonic NDE. It permits accurate, quantitative, noncontact measurement of local displacements normal to the surface of a metal, composite, or ceramic specimen over a wide range of environmental conditions. The interferometer can be internally calibrated to yield absolute displacement amplitudes. With transparent materials, the interferometer can measure internal wave propagation as well. Commonly, the surface displacements are measured at one or more spots [1,2] on the surface — the probe beam can be focused to spots whose diameters range from 0.02 to less than .002mm depending on the f/no of the beam. These temporal records of surface displacement or internal strain correspond to bandwidths limited solely by the electronic amplifier. For the measurements, the surface under test may be polished, at least at the point or points of measurement; alternatively, small 2 x 2 x 0.1mm mirrors can be attached to the surface. But it is possible to make measurements, albeit at lower sensitivity, even if the surface is not polished at all, provided a reasonable amount of light is scattered back into the interferometer.

Laser interferometers can also be used to measure Doppler-shifted scattered light from a very rough surface from which the displacements can be calculated [3]. Yet another technique, heterodyne holographic interferometry [4,5], permits one to make a "snapshot" of an area of the specimen to show an instantaneous picture of the distribution of Rayleigh and impinging bulk wavefronts on the surface.

In this paper, an improved laser interferometer for measuring either surface disturbances or internal disturbances in transparent media is described. The instrument features nearly shot noise limited sensitivity (50pm), displacement measurements (including phase) over a bandwidth of 10MHz, absolute calibration and relative calibration within a millisecond of an event when desirable (i.e. the specimen moves or changes its reflectivity). A few examples of the performance of the instrument are given here; other examples involving low level laser generated signals are described in another paper by E. Bourkoff and C. H. Palmer [6].

LASER INTERFEROMETER

It is well known that interferometry is subject to the "pathlength sensitivity" problem: for best sensitivity, conventional interferometry requires that the round trip optical path difference between the reference and sample beams be fixed at $(m \pm 1/4)$ wavelengths where m is any integer, i.e. the slope of the fringe intensity curve is maximum. This critical pathlength difference is affected by mechanical vibrations, thermal expansion, acoustic noises (which affect the refractive index of air), and, of course, specimen motion. The fringes in a typical commercial Michelson interferometer jitter slightly most of the time. Here we are concerned with displacements as small as 4×10^{-5} wavelength. Various methods have been used to overcome this problem: differential interferometry [7] when continuous ultrasonic waves are to be measured, heterodyne interferometry, the quadrature-dual technique [8,9], and servo control. The interferometer described here is of the latter type.

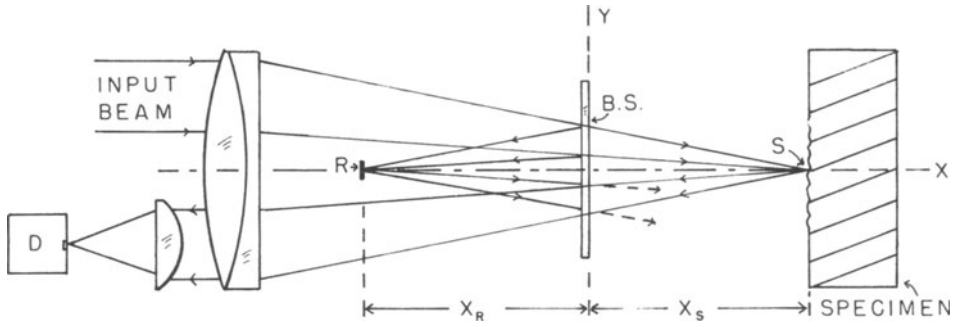

Fig. 1. Basic optical system

A. Basic Optical System

Figure 1 shows the basic optical system of the interferometer. An expanded, collimated laser beam is incident on the larger lens from the upper left, and it is focused on the specimen surface at S. The beamsplitter reflects half the light back to a focus on the reference mirror R. Light reflected both from the specimen and from the reference mirror is recombined at the beamsplitter and directed to the photodetector. Wasted light directed toward the specimen can be used to check the optical alignment.

The in-line design of the interfering optical paths has several advantages: (1) Small torsional oscillations of the interferometer base plate about the x-axis of the instrument, and bending about the x, y, or z axis are all balanced out to first order. (2) Thermal expansions, to first order, have little effect. (3) Acoustic disturbances tend to affect both paths similarly. (4) Very little light is returned to the laser so that an optical isolator is not required to eliminate such light. With this design, the fringe pattern is reasonably stable even without use of the control system.

B. Control System

The interferometer is provided with a control system to further stabilize the residual disturbances in the optical paths and, particularly,

to compensate for the typically much larger specimen motion and vibration problems. It is well known that active electronic components exhibit 1/f noise; that is, they generate more electronic noise at low frequencies than at intermediate frequencies. Thus an ac control system can be expected to suffer less from electronic noise than a dc control system. The ac control system also provides better calibration possibilities.

The output power for two beam interference can be expressed

$$P_o = K(E_r^2 + E_s^2 + 2\,E_r E_s \cos[2k(X_r - X_s) + \phi]) \tag{1}$$

where K is a factor to convert optical intensity to power, E_r and E_s are the reference and sample amplitudes respectively, X_r and X_s the reference and sample paths, k the effective propagation constant in air, and ϕ a phase shift which can be adjusted by varying X_r. If the reference path is sinsusoidally modulated over a small range, its magnitude can be expressed

$$X_r = X_o + A\sin(\omega t) \tag{2}$$

where A is the amplitude of the audio frequency $\omega/2\pi(=3\text{kHz})$. Thus

$$P_o = K(E_r^2 + E_s^2 + 2E_r E_s \cos[2k(X_o - X_s) + \phi - 2kA\sin(\omega t)]) \tag{3}$$

The varying part of this power can be expressed in terms of a fundamental frequency (3kHz), a second harmonic, and higher order terms which are small and may be neglected:

$$P_\omega \propto A\sin(\alpha)\sin(\omega t) \tag{4}$$

$$P_{2\omega} \propto A\cos(\alpha)\cos(2\omega t) \tag{5}$$

$$\alpha = 2k(x_o - X_s) + \phi. \tag{6}$$

For maximum sensitivity we need to make $\phi=\pi/2$ and thus $P_\omega=A\sin(\omega t)$ and $P_{2\omega}=0$. The servo system is therefore designed to null the second harmonic component (6kHz). Note that this component has a different sign, depending upon whether the path difference is too small or too large.

Figure 2 shows a simplified block diagram of the control system. The control element is a piezoelectric tube of PZT material which is fixed at one end and supports the small reference mirror at the other end. A 3kHz oscillator drives the PZT tube to modulate the reference path. In addition the oscillator output is also fed to a frequency doubler and squaring circuit to provide a reference square wave for the synchronous detector (multiplier). The optical output of the interferometer, detected by a photodetector, contains both a video signal (50kHz to 10MHz) and an audio component (3kHz and 6kHz plus harmonics). The 3kHz output, which indicates the relative calibration at any instant, is monitored and can be sampled within a millisecond of any acoustic event. The 6kHz harmonic signal, is fed to the synchronous detector as shown. The detector output, after smoothing, is a dc voltage proportional to the error signal, including sign. This error signal feeds a high voltage dc amplifier which biases the PZT control element so as to correct the optical path error. Since it can easily happen that the required PZT voltage would be either excessively high or else negative, the high voltage is monitored by the over/under switch circuit which momentarily disconnects it from the PZT to permit the system to lock on another fringe for which the voltage is within the allowed range (20 to 150 volts).

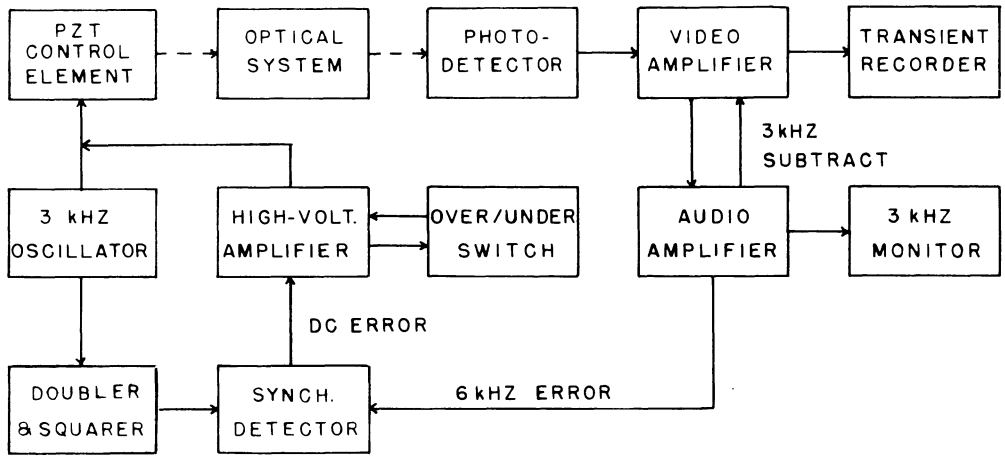

Fig. 2. Simplified Block Diagram of Control System

C. Calibration

Absolute calibration of the interferometer is obtained by driving the reference mirror at a large amplitude at a frequency within the video pass band. For convenience the frequency is approximately 135kHz corresponding to a resonance of the PZT unit. Clearly, as Eq. (1) shows, the maximum change in light level occurs when the argument of the cosine varies from 0 to 180 deg. The curve is, of course, highly non-linear and is described in terms of Bessel functions. The displacement amplitude Δx of an arbitrary waveform is given by

$$\Delta x = (\lambda/2)(v/V_{cal}) \tag{7}$$

where λ is the optical wavelength, v the signal voltage, and V_{cal} is the peak-to-peak calibration voltage.

D. Laser Noise

In a comparison of the laser interferometer performance with that of the capacitive transducer at the National Bureau of Standards, it was found that the interferometer produced an oscillation of about 100kHz frequency superposed on the otherwise correct signal. Investigation showed that laser relaxation oscillations were responsible for the false signal. The effect of these and other sources of laser power fluctuations can be essentially eliminated by dividing the input laser beam into two orthogonally polarized components which are made to be 180° out of phase with each other. Two photodetectors sense these two orthogonally polarized components, and their outputs subtracted. If there is an optical path change, the subtracted signals yield the same final voltage, and hence twice the signal of one beam alone. There is, of course, no net gain here since each beam has only half the power of the unmodified optical system. Any momentary increase in laser output power, however, is now subtracted out so that it has negligible effect. In reality, since the laser power multiplies the signal power, the power fluctuation is still present, but now, for a 1% change in signal power, it modulates the signal amplitude by 1% instead of producing a false signal which may dominate the signal to be observed.

Figure 3 shows the modified optical system with the two outputs and the slight modification to the electronics. Figure 4 shows the effectiveness of this technique. In the lower curve, the laser input beam power was

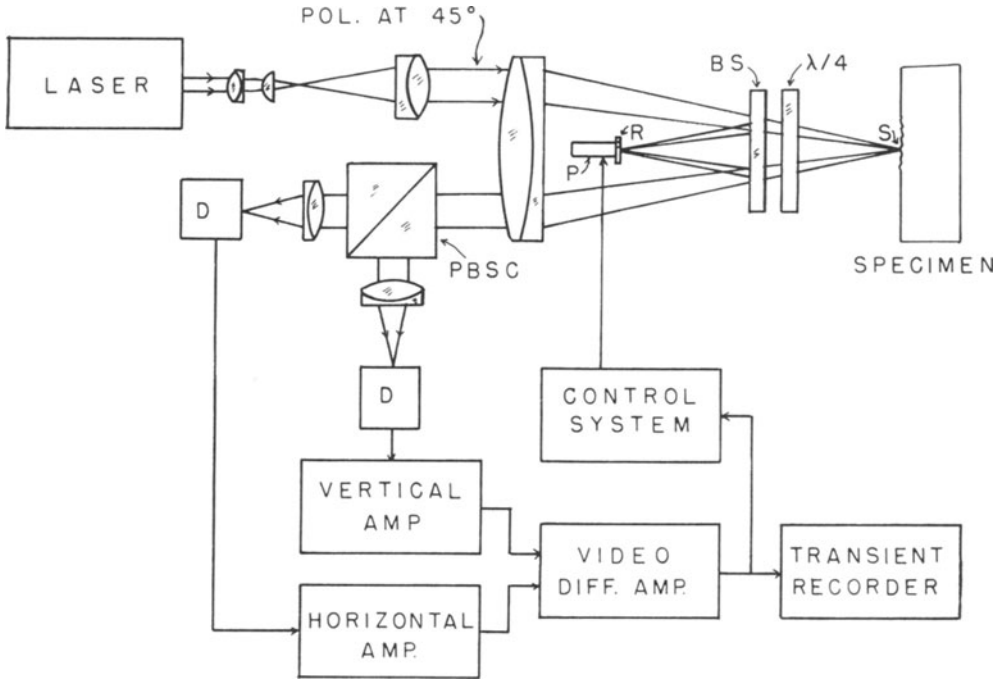

Fig. 3. Arrangement to remove laser relaxation oscillations by subtraction of two out-of-phase signals

modulated at 156kHz by driving a knife edge into the beam at a focal point using a piezoelectric device. At the same time, the sample optical path was sinusoidally modulated at 30kHz by a second piezoelectric device. The amplitudes were adjusted so that they were both reasonably large and about equal in magnitude. The lower curve shows the output of one channel of the interferometer; the upper curve shows the difference signal video output. Note that the removal of the power level variation is incomplete. When this recording was made, it was found that the electronic subtraction was inadequate because of a small time delay in the two signal channels. When a good differential amplifier circuit is used, the subtraction is much better, and the errors in the subtracted signals are essentially absent.

PERFORMANCE

The accuracy with which the actual displacement waveform was reproduced was tested in a series of experiments in which seismic events were generated by breaking glass capillaries on the axis on one side of various discs. The normal surface displacements directly opposite, on the other side, were measured. In the first experiment, a 6061T6 aluminum disc 152mm dia. and 63.4mm thick was used. The purpose was to compare the waveform recorded by the interferometer and by a commercial piezoelectric transducer. To make possible simultaneous recording, the piezoelectric transducer was offset 15mm on one side of the cylinder axis and the interferometer probe spot an equal amount on the other side of the axis. The results were totally different. The piezoelectric transducer responded well to the arrival of the P, S, and PPP waves. The signals, however, were delayed about a microsecond (presumably the travel time of the wave through the wear plate), and they did not indicate displacement information directly. The optical signal, on the other hand, yielded a waveform that corresponded well to the theoretically expected signal up to the time when an edge-reflected P wave arrived. The theory assumes a slab of infinite dimension and hence does not account for such waves.

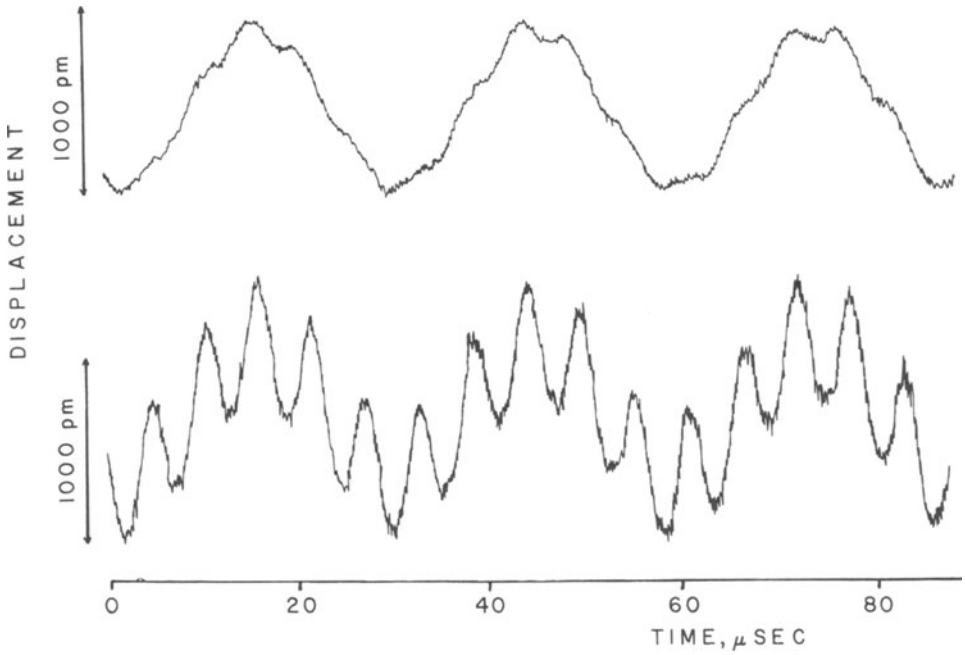

Fig. 4. Effectiveness of laser noise removal. The Lower curve is artificial, large 156kHz sinusoidal "noise" superposed on 30kHz sinusoidal signal. The Upper curve shows the noise removed (mostly) and the 30kHz "true" signal remaining.

For a better comparison with theory, a similar seismic event was generated in a thinner disc, 25.4mm thick, on axis. For this disc, unlike the thicker one, edge reflected waves do not arrive until after the direct P,S, and PPP waves have been detected. This time the optical signal was detected on axis. Figure 5 shows the recorded optical signal (solid line) and the theoretical response (dashed line) after Knopoff [10]. The main difference between theory and experiment is the gradual rise in the optical signal as compared to predicted step rise. The electronic bandwidth for the interferometer, 10MHz, precludes such an abrupt rise. Also, the glass capillary does not break instantly either.

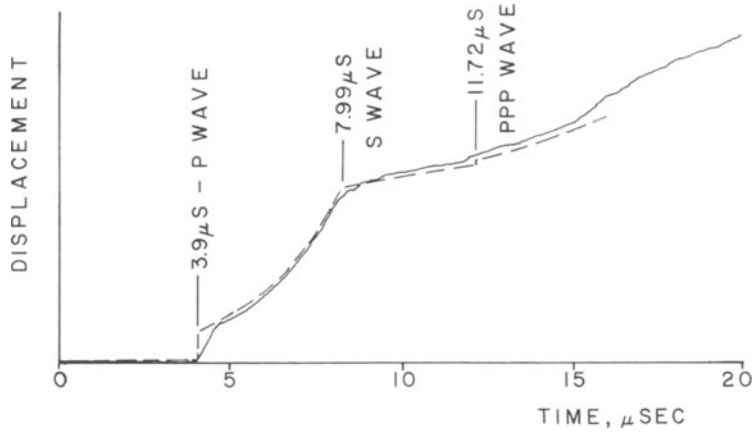

Fig. 5. Measured (solid) and Theoretical (dashed) normal displacement waveforms for seismic event at epicentral point on 25.4mm thick disc.

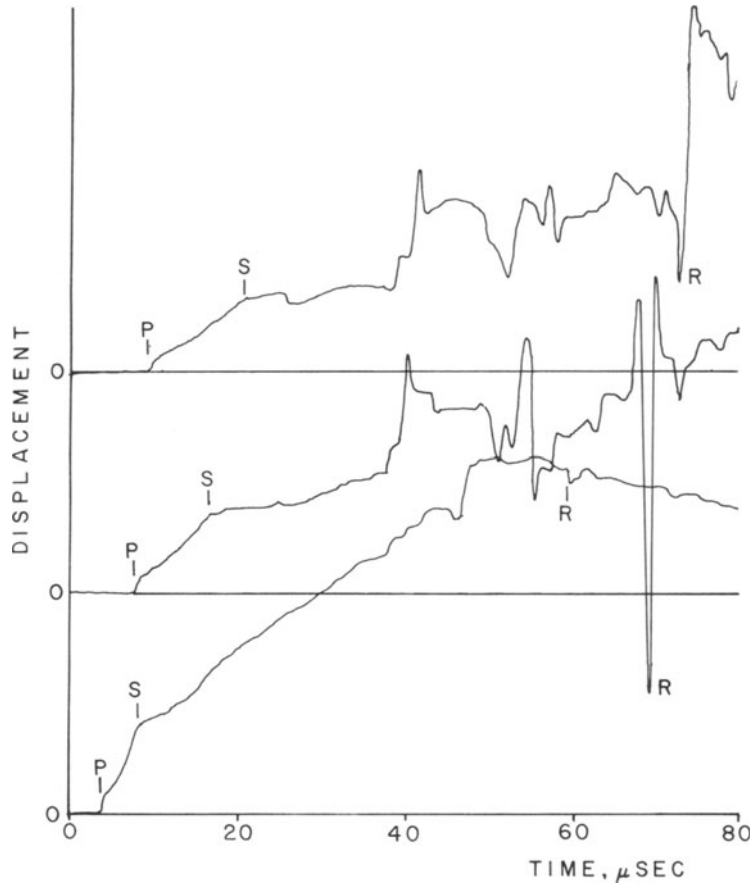

Fig. 6. Normal displacement waveforms for three 152.6mm. dia. aluminum discs. Upper curve 63.1mm thick; middle curve 50.8mm thick, lower curve 25.4 mm. thick (same disk as Fig. 5).

Figure 6 shows the arrival of various waves, direct and indirect for three 6061T6 aluminum discs, all 152.6mm dia. and of various thicknesses. The upper curve resulted for a thickness of 63.5mm, the middle curve for 50.8mm, and the lowest curve for a thickness of 25.4mm. The first waves to arrive in all cases were the P and S waves. In the two upper curves the next arrival is a longitudinal wave reflected from the side of the cylinder to the point of observation, followed by the PPP wave and then various other waves including mode converted waves and a Rayleigh wave which propagates radially from the center to the edge, down along the edge, and radially inward to the observing point. It is interesting to note the big differences in displacement observed. There are various possible explanations for these differences, but the right explanation has not yet been identified.

In another experiment the seismic event was generated on a glass disc 49.5mm thick, 170mm diameter. (The disc was actually not a cylinder, but effectively two cylinders of different diameter cemented together. An interesting feature was that, because the disc was transparent, some of the laser light of the interferometer probe beam was transmitted to the glass capillary and scattered back to the photodetectors. Thus when the capillary broke, the level of this scattered light changed and gave rise to a signal corresponding to $t=0$. The remainder of the trace is very similar to the aluminum traces except for wave speeds.

In the paper by Bourkoff and Palmer [6], as mentioned above, we show laser generated waveforms generated in aluminum and two composites which were detected by this interferometer. In that paper we include quantitative displacement information. (In the examples above, the displacement amplitudes were not measured — they were of the order of several thousand picometers.)

CONCLUSION

A servo controlled interferometer of new design has been described and its performance illustrated. The sensitivity is within a factor of two or three of shot noise limitation. Additional features include absolute calibration, instantaneous relative calibration, adjustable bandwidth determined by the video amplifier, and ability to measure waveforms with no loss of phase information.

This work has been made possible by the Armstrong gift fund for Nondestructive Evaluation.

REFERENCES

1. C. H. Palmer and R. E. Green, Jr., Appl. Opt. 16, 2334 (1977).
2. C. H. Palmer and R. E. Green, Jr., "Optical Probing of Acoustic Emission Waves," Final Report, U.S. Army Research Office, Durham, NC, Aug. 31, 1979, Grants No. DAAG-29-76-G-0160; DAAG-29-78-G-0050.
3. J. P. Monchalin, Appl. Phys. Lett. 47, 14 (1985); (see also these proceedings).
4. R. Danliker, in Progress in Optics, E. Wolfe, ed., Vol. 17, 1-88 (1980).
5. J. W. Wagner, Appl. Opt. (to be published).
6. E. Bourkoff and C. H. Palmer, "Noncontact Material Testing Using Low Energy Optical Generation and Detection of Acoustic Pulses," (These proceedings).
7. C. H. Palmer, R. O. Claus, and S. E. Fick, Appl. Opt. 16, 1849 (1977).
8. E. R. Peck and S. W. Obetz, J. Opt. Soc. Am. 43, 505 (1953).
9. D. Vilkomerson, Appl. Phys. Lett. 29, 183 (1976).
10. L. Knopoff, J. Appl. Phys., 29, 661 (1956).